การพัฒนาเส้นใยนาโนที่มีอนุพันธ์ของ โรดามีน บี เป็นองค์ประกอบเพื่อใช้เป็นตัวตรวจวัดทางเคมีเปลี่ยนสีสำหรับการตรวจวัดคอปเปอร์ (II) ไอออน

Development of Nanofibers Containing Rhodamine B as Colorimetric Chemosensor for Cu^{2+} Determination

มาธิตา ร่มโพธิ์[1], สรายุทธ เวชสิทธิ์[2], อภิชาติ อิ่มยิ้ม[3] และ จอมใจ สุกใส[1*]

Mathita Rompo[1], Sarayut Watchasit [2], Apichat Imyim[3] and Chomchai Suksai[1*]

[1] *ศูนย์ความเป็นเลิศด้านนวัตกรรมทางเคมี ภาควิชาเคมี คณะวิทยาศาสตร์ มหาวิทยาลัยบูรพา*

[2] *ห้องปฏิบัติการนิวเคลียร์แมกเนติกเรโซแนนซ์สเปกโตรมิเตอร์ คณะวิทยาศาสตร์ มหาวิทยาลัยบูรพา*

[3] *ภาควิชาเคมี คณะวิทยาศาสตร์ จุฬาลงกรณ์มหาวิทยาลัย*

[1] *Department of Chemistry and Center for Innovation in Chemistry, Faculty of Science, Burapha University*

[2] *Nuclear Magnetic Resonance Spectroscopic Laboratory, Faculty of Science, Burapha University*

[3] *Department of Chemistry, Faculty of Science, Chulalongkorn University*

Received : 31 May 2018

Accepted : 12 July 2018

Published online : 1 August 2018

บทคัดย่อ

ในงานวิจัยนี้ ได้ทำการเตรียมเซ็นเซอร์ทางเคมีเชิงแสงจากเส้นใยนาโนของเซลลูโลสอะซิเตท CA ที่มีอนุพันธ์ของโรดามีน บี L1 เป็นองค์ประกอบโดยใช้เทคนิคอิเล็กโตรสปินนิงเพื่อนำมาใช้ในการตรวจวัดคอปเปอร์(II) ไอออน จากการศึกษาลักษณะทางสัณฐานวิทยาของเส้นใยนาโนดังกล่าวด้วยเทคนิค SEM พบว่าเส้นใยที่เตรียมได้มีขนาดเส้นผ่านศูนย์กลาง 92 ± 24 นาโนเมตร นอกจากนี้ยังพบว่าเซ็นเซอร์ทางเคมีเชิงแสงจากเส้นใยนาโนที่เตรียมได้มีความจำเพาะเจาะจงกับคอปเปอร์(II) ไอออนเป็นอย่างดี โดยในสภาวะที่มีคอปเปอร์(II) ไอออนอยู่ในระบบของเส้นใยจะเปลี่ยนจากสีชมพูจางเป็นสีชมพูเข้ม อันเป็นผลเนื่องมาจากการเกิดสารประกอบเชิงซ้อน CuL1 ภาวะที่เหมาะสมในการตรวจวัดคอปเปอร์(II) ไอออนด้วยเส้นใย L1-CA คือใช้ปริมาณ L1 ที่ 25 มิลลิกรัม สารละลาย pH เท่ากับ 5 และเวลาที่ใช้ในการตรวจวัดคือ 20 นาที โดยมีค่าขีดจำกัดต่ำสุดของการตรวจวัดคอปเปอร์(II) ไอออน เท่ากับ 1.62 mg L^{-1}

คำสำคัญ : เส้นใยนาโน, เซลลูโลสอะซิเตท, คอปเปอร์(II)ไอออน, โรดามีน บี, อิเล็กโตรสปินนิง

* Correspondent author. E-mail : jomjai@buu.ac.th

Abstract

In this work, a visual colorimetric sensor based on cellulose acetate nanofibers incorporated with rhodamine B hydrazone derivative **L1** was successfully prepared via electrospinning technology. Morphology of the nanofibrous sensor was characterized by SEM, which showed that the uniform nanofibers having diameter of 92 ± 24 nm and formed a non-woven mat. The prepared colorimetric nanofibers showed high sensitivity towards Cu^{2+} due to the color change from pale pink to intense pink which confirmed the formation of **CuL1** complex ion in **L1-CA** nanofibers. Upon the optimal conditions of amount of **L1** at 25 mg, pH solution at 5.0 and response time of 20 min, the detection limit for Cu^{2+} with **L1-CA** nanofibers was found to be 1.62 mg L^{-1}.

Keywords : nanofibers, cellulose acetate, copper(II)ion, rhodamine B, electrospinning

Introduction

Copper is the third-most abundant transition metal in the human body and also has been used as catalytic cofactors for various types of metalloproteins for example superoxide dismutase, cytochrome c oxidase and tyrosinase (O'Halloran & Culotta, 2000; Crichton *et al*., 2008; Nunes *et al.,* 2015). Accumulated Cu^{2+} ions in the body in high amount through drinking water can be harmful and toxic to our biological system (Ahuja *et al*., 2015; Miotto *et al.,* 2014; Strausak *et al.,* 2001; Telianidis *et al.,* 2013; Jensen *et al.,* 1999). According to WHO, the limit of concentration of Cu^{2+} ions in drinking water is 2 mg/L (WHO., 2017). Because of these potential hazards, it is essential to control and measure the Cu^{2+} ions for protection of our environment and health.

Several analytical techniques such as atomic absorption spectrometry (AAS) (Pourreza & Hoveizavi, 2005), inductively coupled plasma atomic emission spectrometry (ICP-AES) (Liu et al., 2005), electrochemistry (Flores *et al.,* 2017) and colorimetric methods have employed for determination of Cu^{2+}. Among them, a colorimetric method shows simplicity, convenience, low-cost and easy way to detect Cu^{2+} by naked-eye without the use of any sophisticated instrument (Piriya *et al.,* 2017; McDonagh *et al.,* 2008).

As already known, rhodamine derivatives are non-fluorescent and colorless, whereas ring-opening of the corresponding spirolactam gives rise to strong fluorescence emission and a pink color. Due to their outstanding optical characteristics, rhodamine derivatives have been often employed and exploited as fluorescent and colorimetric chemosensors for metal ions and anions (Kim *et al.,* 2008; Chen *et al.,* 2012). It should be noted that all of these synthetic sensing molecules are insoluble in water due to their hydrophobic in nature, however in real samples most of analysis target samples dissolves in water. Therefore, it would be a challenge to fabricate the sensing materials by incorporation of rhodamine derivatives into suitable solid support materials and apply as naked-eye sensor for selective sensing of interested target analytes.

Various types of sensing materials from rhodamine and its derivatives have been fabricated. For example, Felpin and co-workers have modified cellulose paper by anchoring rhodamine B derivative and applied this device for detection of hydrogen sulfate anions (Felpin *et al.,* 2016). Ozay and co-workers have developed rhodamine based hydrogel for sensing Fe^{3+} (Ozay & Ozay, 2013). Xie and co-workers have immobilized rhodamine 6G on surface of SiO_2 nanoparticles which exhibited the high sensitivity and selectivity for Hg^{2+} (Liu *et al.,* 2013). Li and co-workers have modified graphene oxide sheets and dispersed into rhodamine B solution. It was found that this material showed the highly selective sensing for Fe^{3+} (Zhang *et. al.*, 2018).

Nowadays, nanofibrous membrane became a more attractive attention due to their high surface area to volume ratio and high porosity material. Various methods for nanofiber production are reported for example drawing-processing, template-assisted synthesis, self-assembly, solvent casting and phase separation (Terra *et al.*, 2017). However, one of the most cost-effective techniques is electrospinning. Not only provides non-wovens few nanometers fibrous membrane, but also electrospinning could produce the thin fibers in large scale production. In order to provide nanofibrous sensors, various types of support polymers for their immobilization have been employed. Remarkably, several colorimetric sensors from electrospun nanofibers with various types of synthetic polymers and biopolymers support have been reported (Chen *et al.,* 2015; Wu & Lai, 2016; Saithongdee *et al.*, 2014; Hu *et al.,* 2017). .

Tong and co-workers reported that the rhodamine B derivative **L1** could be used as colorimetric sensor for Cu^{2+} in 50% (v/v) water/CH_3CN at 10 mM Tris-HCl pH 7.0 (Xiang *et al.,* 2006). It was found that addition of Cu^{2+} to the solution of **L1** resulted in the ring-opening of the spirolactam moiety giving **CuL1** as complex adduct concomitantly to the color change from colorless to pink color. The change in chemical structure of Cu^{2+} sensing by **L1** was depicted in Figure 1. Therefore, this research work aimed to fabricate colorimetric naked-eye sensor for Cu^{2+} in aqueous solution from cellulose acetate (CA) electrospun nanofiber using the rhodamine B hydrazone derivative **L1** as a chemical sensor.

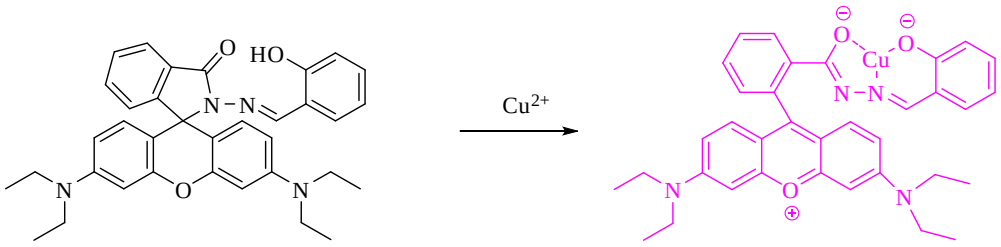

L1 **CuL1**

Figure 1 Change in chemical structure of Cu^{2+} by **L1**.

Methods

Chemicals

Cellulose acetate (CA, Mn ~30,000) was purchased from SIGMA-ALDRICH. N,N-Dimethylacetamide (DMAc,) and acetone (AR) were ordered from LABSCAN. All other chemicals are analytical grade and used without further purification.

Synthesis of the rhodamine dye L1

The rhodamine dye **L1** was facilely synthesized from rhodamine B by a two-step reaction according to the method reported in the literature (Xiang *et al.,* 2006).

Preparation of L1-CA colorimetric nanofibers

Before electrospinning, the CA polymer (20 %wt) solution and **L1** (15 – 35 mg) was stirred together in a mixture solvent of acetone: DMAc (3:2, v/v) at room temperature for 15 h. Next, the polymer mixture was loaded in a 5 mL syringe which was placed onto a syringe pump (NE-1000, ProSense B.V.). The mixture was spun under an electrical field of 14 kV by a high voltage power supply (EQ-30P1-L(230V), Matsusada Precesion Inc). The distance between the needle and the collector was 14 cm and the flow rate used was 0.2 mL/h. Electrospinning in this work was performed in horizontal alignment having a grounded aluminum foil which serves as a collector.

Characterization methods

The morphology and diameter of nanofibers were determined by SEM (Model LEO 1450VP). The SEM image was recorded at the magnifications of 15,000. The average diameter and its standard deviation (n = 40) of the electrospun fibers were determined by image J soft-ware. (National Institute of Health, USA). To investigate the functional groups presented on the nonofibers, an attenuated total reflectance Fourier transform (ATR-FTIR) spectrometer (PerkinElmer-Frontier) was used to record the IR absorption in the range of wavenumber between 4000–400 cm^{-1} and a resolution of 4 cm^{-1}.

Water contact angles were measured with a sessile drop method by a DCA 20 contact angle meter (Data Physics Co., Ltd., Germany). The angles between the water droplet (2 µL) and the surface were measured. The measurement used distilled water as the reference liquid and it was automatically dropped on the electrospun scaffolds. To contact angle was measured in triplicates from different positions and an average value was calculated by a statistical method.

For sensing studies of nanofibrous sensor, all of experiments have been performed in 5 replicates. Before color analysis for metal ion sensing, the nanofibers were air dried for 30 minutes to allow the formation of a stable color and complete drying. Thereafter, the image of nanofibers was measured using a CanoScan LiDE 25 scanner and analyzed the intensity by Image J program (National Institute of Health, USA).

Results and Discussion

Sensing abilities of L1 with metal ions

The sensing abilities of **L1** towards metal ions were investigated by UV-vis spectrophotometry in CH_3CN/H_2O mixture (1:1, v/v). As already known, metal ions could induce ring opening of the spirolactam moiety in rhodamine structure resulted in the color change from colorless to deep pink or purple color. Therefore, after addition of various metal ions to the solution of **L1** (10 μM) , only Cu^{2+} changed the color of **L1** solution from colorless to intense pink color whereas other metal ions such as Cr^{3+}, Fe^{3+}, Ni^{2+}, Zn^{2+} and Hg^{2+} showed a negligible change in color, as seen in Figure 2(a). These results are agreed with the UV-Vis spectrum of **L1** in the presence of various metal ions as shown in Figure 2(b). The addition of Cu^{2+} to the solution of **L1** obviously causes the appearance of a new peak at 558 nm assigned to the internal charge transfer process. Therefore, **L1** could not sense Cu^{2+} selectively in a mixture of organic/aqueous medium.

(a)

(b)

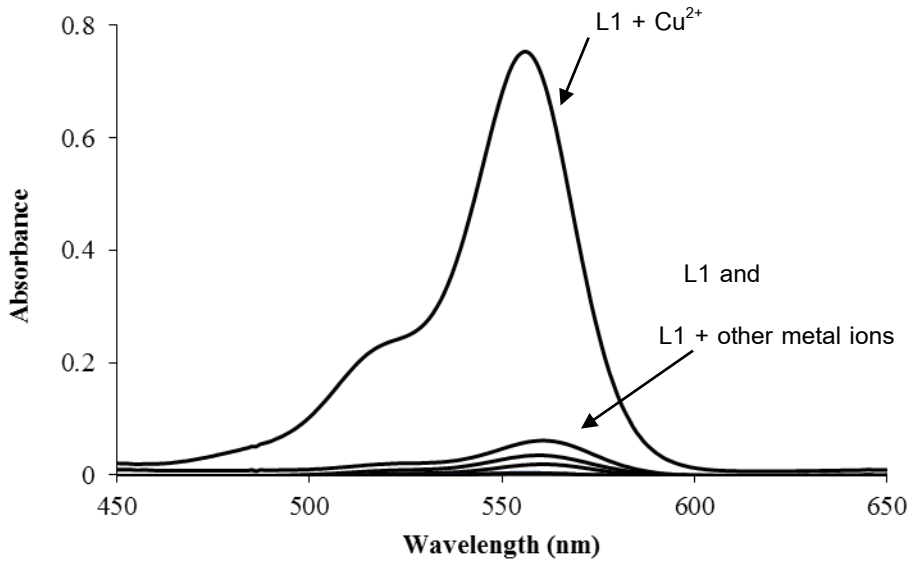

Figure 2 (a) The photograph and (b) the UV-Vis spectra of **L1** (10) μM in the presence of various metal ions (10 eq.) in 50%(v/v) H_2O/CH_3CN.

Characterization of the L1-CA nanofibers

A typical SEM image of CA and **L1-CA** nanofibers are shown in Figure. 3. The average diameter (D) of nanofibers was estimated by the equation (1):

$$D = \frac{1}{n}\sum_{i=1}^{n} X_i * \frac{B}{L} \qquad (1)$$

where n stands for the number of the nanofibers in SEM images, X stands for the diameter of each nanofiber, B is the scale bar, and L refers to the length of the scale bar (Wang et al., 2011). In Figure 3, the morphology of both nanofibers showed satisfactory fiber mats observed by smooth and straight fibers. The average diameter of electrospun CA nanofibers and **L1-CA** nanofibers were 87 ± 15 nm and 92 ± 24 nm (mean ± S.D., n = 40), respectively.

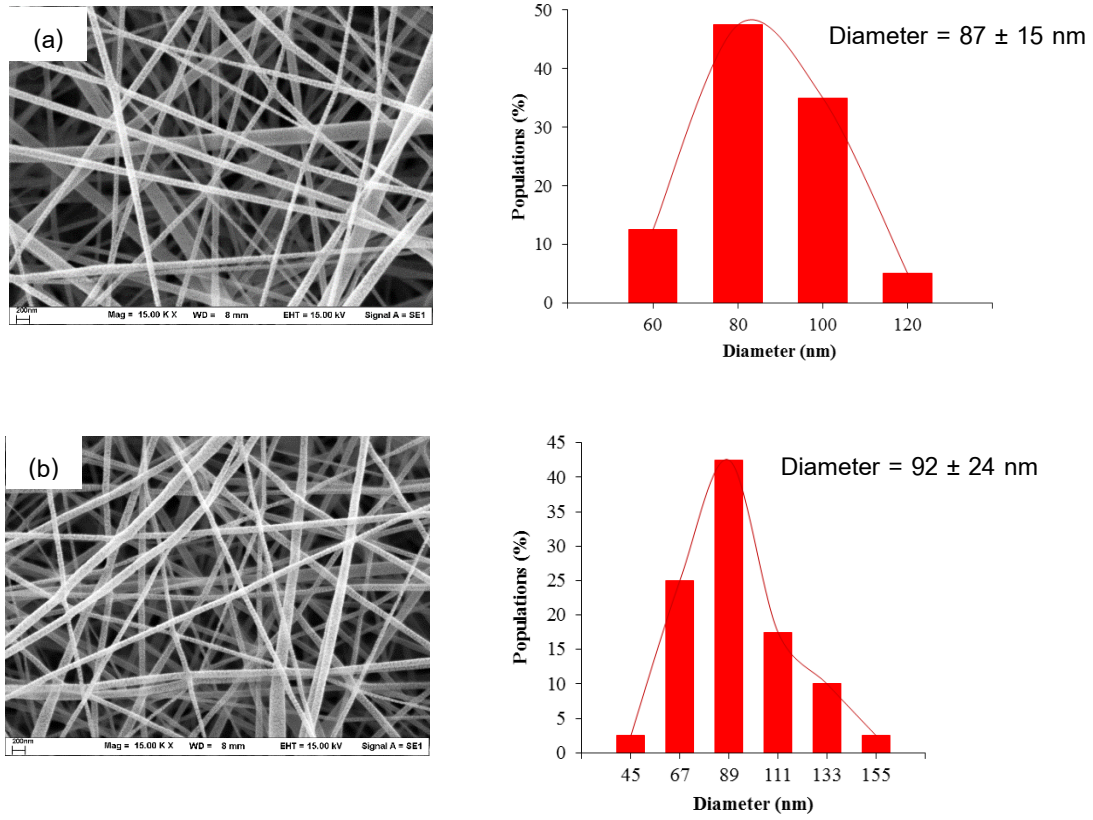

Figure 3 SEM images and diameter distribution diagram of **(a)** CA nanofibers and **(b)** **L1-CA** (**L1** = 25 mg) nanofibers.

ATR-FTIR spectra of **L1**, CA, and **L1-CA** nanofibers are presented in Figure 4. CA showed the vibrational peak at 1743 cm^{-1} and 1426 cm^{-1} corresponded to C=O stretching of acetyl group and the asymmetric vibration of CH_3 group in CA Figure 4(a). The **L1** powder showed the several characteristic medium or strong peaks at 2932, 1720 and 1613 cm^{-1} vibration referred to CH_3 or CH_2, C=O and C=N vibrations, Figure 4(b) (Wang *et al*., 2017). The ATR-FTIR spectrum of the electrospun **L1-CA** membrane (Figure 4(c)) exhibited very similar characteristic absorption to those of CA nanofibers. This indicated that in the presence of **L1** the electrospinning process did not alter the structure of CA in **L1-CA** membrane. It should be noted that the characteristic absorption bands of **L1** were not observed probably because it was loaded into the membrane at a low ratio of 1.25 %w/w of CA .However, the membrane showed a pale-pink color of **L1** which was significantly different from the free CA membrane.

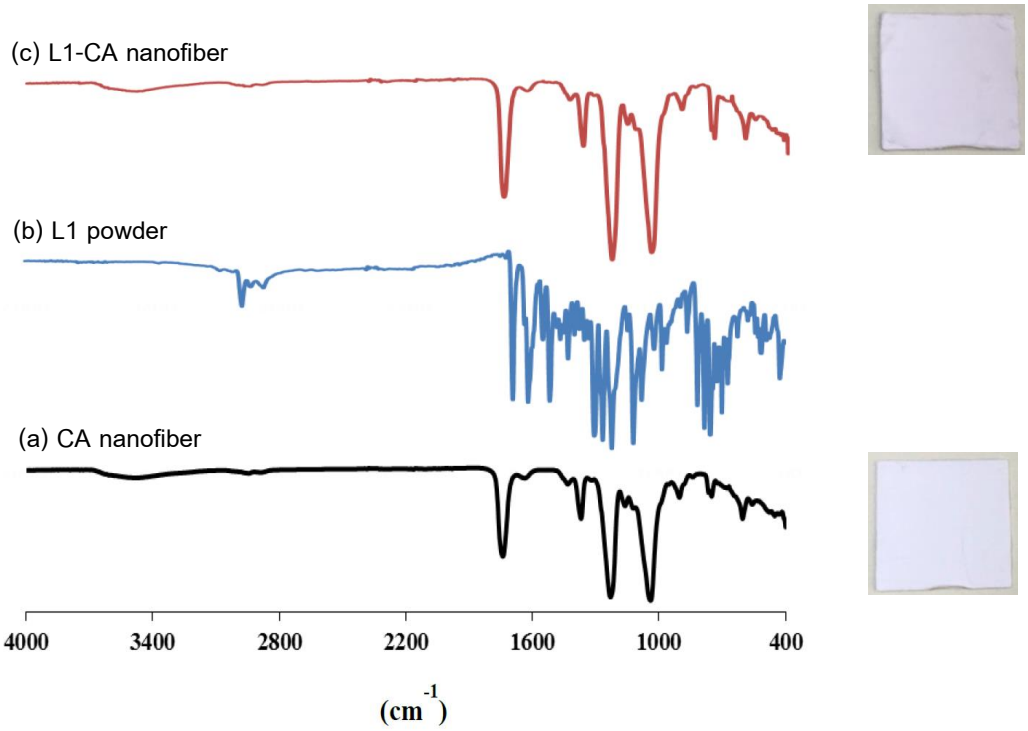

Figure 4 ATR-FTIR spectra of **(a)** CA nanofibers, **(b) L1** powder and **(c) L1-CA** nanofibers.

The elemental composition on the surface of modified fibers was further investigated by energy dispersive X-ray spectroscopy (EDX). It was found that increasing amount of nitrogen in the spectrum of **L1-CA** nanofibers compared to CA nanofibers could confirm the participation of **L1** in **L1-CA** nanofibers (data not shown).

Optimization of Cu^{2+} sensing by L1-CA nanofibers

The optimization of conditions for sensing Cu^{2+} by **L1-CA** nanofibers are performed by the study of amount of **L1**, optimum pH and response time. The composition of the nanofibers with respect to **L1** was optimized by preparing the samples having different amounts of **L1** from 15, 20, 25, 30 and 35 mg in 20 wt% CA solution. After immersion of fabricated **L1-CA** nanofibers to Cu^{2+} solution, it was found that by increasing amount of **L1** the intensity of pink color on nanofibers increased up to 25 mg, and then the color intensity was insignificantly decreased as shown in Figure 5(a). It could be rationalized that the decreasing of intensity might be related to the large amount of hydrophobic **L1** molecule in CA nanofibers resulting in minimization of Cu^{2+} exchange form solution. Therefore, the amount of the **L1** in the nanofibers was fixed to 25 mg for further studies. Changing in color of **L1-CA** nanofibers from colorless to pink confirmed that Cu^{2+} could induce the formation of the ring opening of the spirolactam moiety in **L1** corporated in **L1-CA** nanofibers. SEM image showed that the mean diameter of **L1-CA** nanofibers after immersion to Cu^{2+} solution was found to be 96 ± 10 nm, Figure 5(b). The presence of **CuL1** complex was confirmed by EDX spectra (Figure 5(c)).

(a)

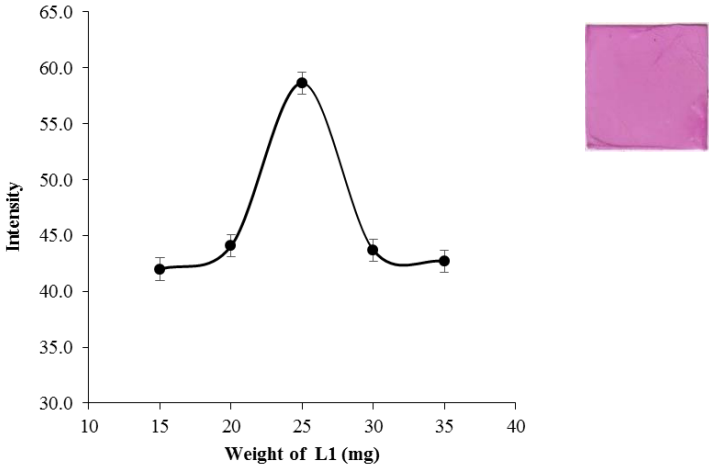

(b)

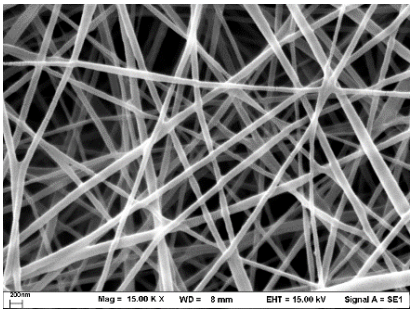

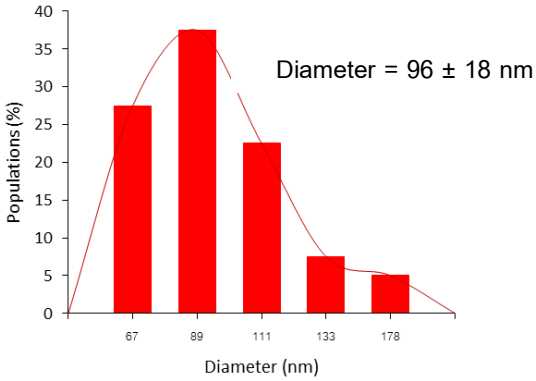

(c)

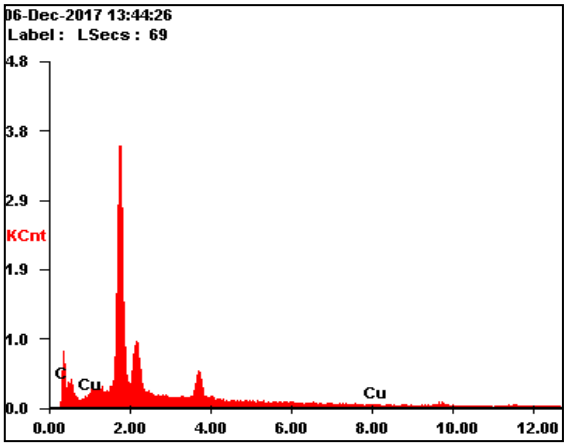

Figure 5 (a) The optimum of L1 amount in L1-CA nanofibers, (b) SEM image and diameter distribution diagram of L1-CA nanofibers (L1 = 25 mg) after immersed into Cu^{2+} 200 ppm solution and (c) EDX spectra for L1-CA nanofibers after immersed into Cu^{2+} 200 ppm solution.

To investigate the surface properties of nanofibers, water contact angles were measured and shown in Figure 6. The bare CA nanofibrous membrance showed an angle around 121°(Figure 6(a)) indicating that CA nanofibrous scaffolds were hydrophobic. The water contact angle of **L1-CA** nanofiber increased to 124° (Figure 6(b)) indicated that the hydrophobic property of **L1-CA** nanofibers are increased due to the presence of hydrophobic **L1** molecule. Interestingly, after the immersion of **L1-CA** nanofiber to Cu^{2+} solution the contact angles decreased to 12.7° (Figure 6(c)), implying that the nanofibers transformed to be hydrophilic. This observation could reveal the formation of **CuL1** complex fromed in nanofibers that led to increasing of the membrane hydrophilicity.

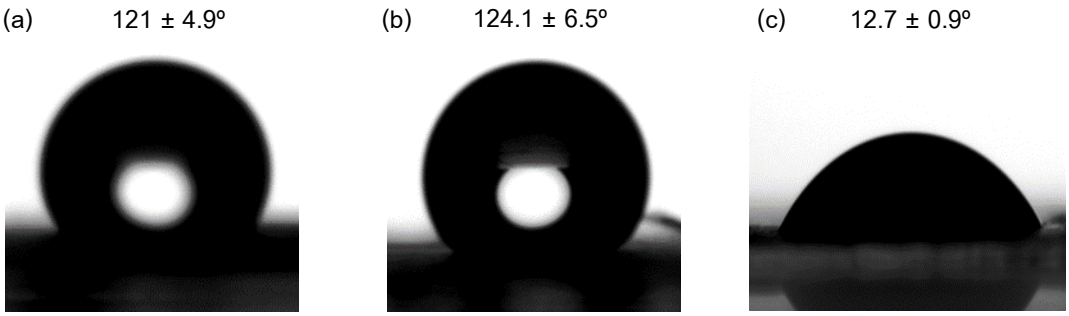

Figure 6 Contact angle images of **(a)** 20% wt CA nanofibers, **(b) L1-CA** nanofibers and **(c) L1-CA** nanofibers (**L1** = 25 mg) after immersion to Cu^{2+} solution.

In order to select the optimum pH value for Cu^{2+} naked-eye sensing, the influence of the pH of the medium was studied over the pH range of 3.0 - 5.0. Figure 7 shows the influence of pH on the intensity of the **L1-CA** nanofibers after immersion to Cu^{2+} solution. It was found that the intensity of pink color increased when pH increased from 3 to 5 and then it became decrease. The decreasing in the intensity at higher pH values can be attributed to the formation of stable copper hydroxide in the solution. Therefore, the pH of the solutions at 5 was chosen in the rest of experiments.

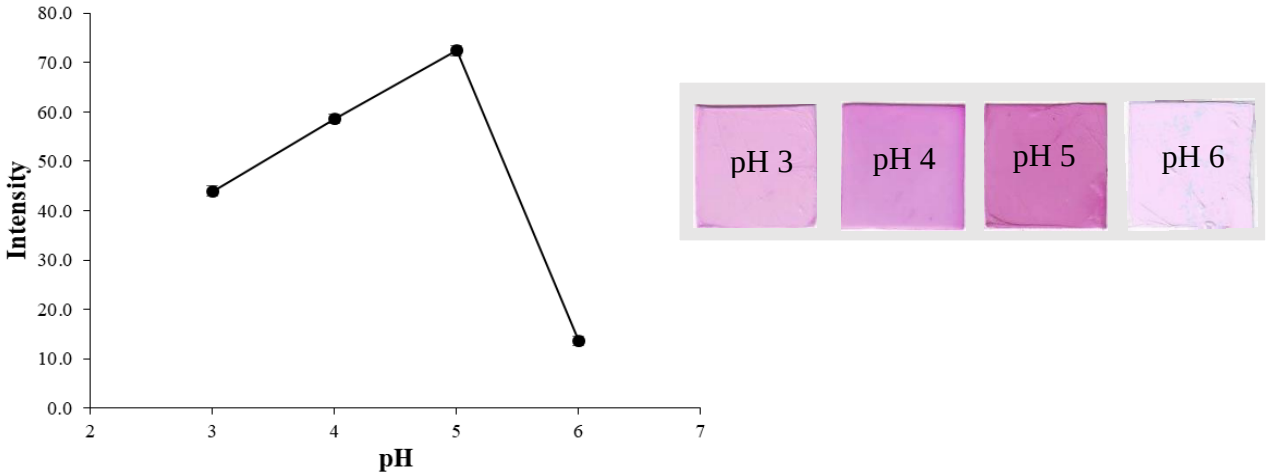

Figure 7 Effect of pH for detection Cu^{2+} (200 ppm) by **L1**-CA nanofibers with corresponding color changed in nanofiber image.

Response time for the colorimetric detection of Cu^{2+} by **L1-CA** nanofibers was studies by immersion of **L1-CA** nanofibers in Cu^{2+} solution at 200 ppm with various times. It can be seen in Figure 8, that at 20 minutes the highest intensity was observed. However, after 20 minutes the intensity was decreased probably due to the leaching of hydrophilic **CuL1** species from nanofibers. These results are agreed well with the results from contact angle experiments.

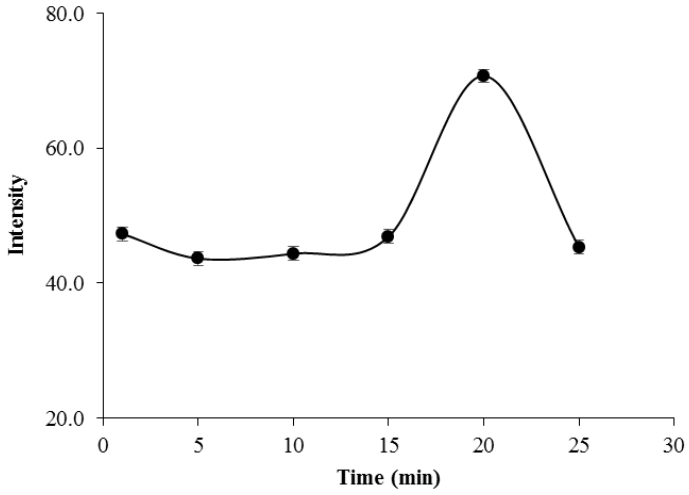

Figure 8 Response time for the colorimetric detection of Cu^{2+} by **L1-CA** nanofibers.

The selectivity of the **L1-CA** nanofiber as metal ion sensor was evaluated with various metal ions such as Mn^{2+}, Fe^{3+},Co^{2+}, Ni^{2+},Cu^{2+}, Zn^{2+},Cd^{2+}, Hg^{2+} and Pb^{2+} at concentration of 200 ppm and pH 5. Figure 9 shows that only Cu^{2+} could change the color of **L1-CA** from colorless to pink. Visually, no significant color changes were promoted by other studied metal ions. Therefore, **L1-CA** nanofibers could be an excellent naked-eye sensor for the detection Cu^{2+} in water at pH 5.

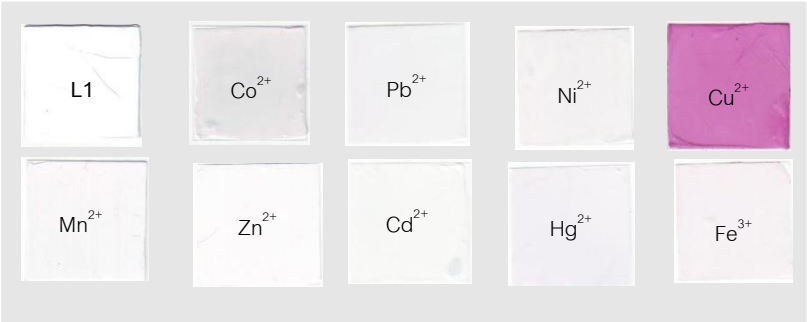

Figure 9 Selectivity of **L1-CA** nanofibers in the presence of various metal ions (200 ppm) at pH 5.

L1-CA nanofibers were tested for colorimetric response with Cu^{2+} in different concentrations. The nanofibers were immersed into various concentrations of Cu^{2+} at pH 5 for 20 minutes and kept for observation at room temperature for 30 minutes. Figure 10(a), the color of **L1-CA** nanofibers were changed from colorless to pink with increasing amount of Cu^{2+} from 1 – 300 ppm. Notably, the intensity of pink color on **L1-CA** nanofibers were found to increase as a good linear relationship with the concentration of Cu^{2+} between 1 – 10 ppm, R^2 = 0.9958. The result suggested that **L1-CA** nanofibers was potentially applicable for quantitative analysis of Cu^{2+} ion in water.

(a)

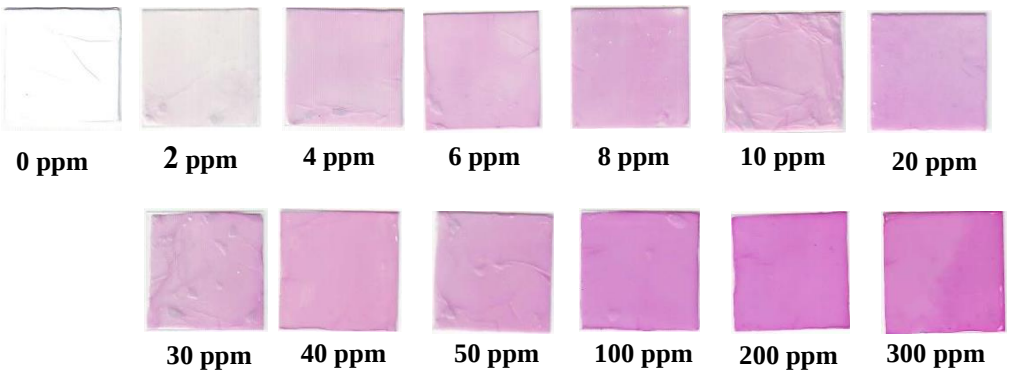

(b)

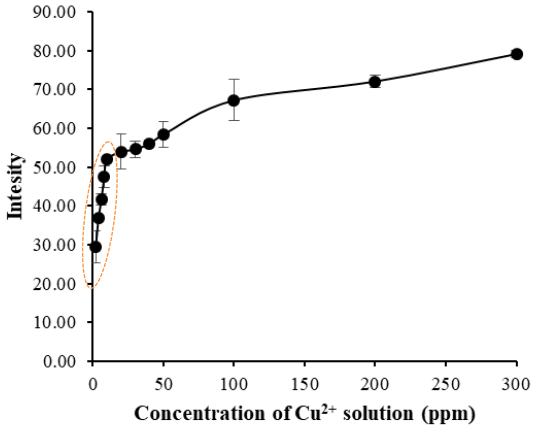

(c)

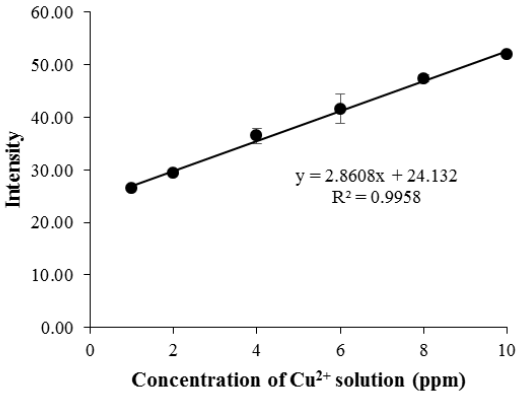

Figure 10 (a) The color changes of L1-CA nanofibers when increased concentration of Cu^{2+} from 1 – 300 ppm at pH 5 , (b) the responses curve between intensity and different concentration of Cu^{2+} from 1 - 300 ppm at pH 5 and (c) the linear dependence concentration between intensity and different concentration of Cu^{2+} from 1 - 10 ppm at pH 5.

The limit of detection (LOD) determines the sensitivity of the method. LOD is the lowest concentration of analyte in a sample which can be detected. LOD was calculated by equation (2);

$$LOD = 3\delta / s \qquad (2)$$

where δ is the standard deviation and *s* is the slope of calibration (Busaranon *et al.*, 2006). The standard deviation was calculated from the slope of the calibration curve. The limit of detection (LOD) of the proposed method was found to be 1.62 mg L^{-1}. The method was found to have a detection limit lower than the WHO guideline limit (2 mg L^{-1}) for Cu^{2+} in drinking water.

The prepare nanofibrous sensing materials was applied to determine Cu^{2+} in synthetic waste water from our laboratory and the results are shown in Table 1. As can be seen from the table, **L1-CA** nanofibers could be applied to detect Cu^{2+} in water samples.

Table 1 Analysis of Cu^{2+} in waste water from our laboratory.

Sample	Concentration added (ppm)	Concentration from AA (ppm)	This work (ppm)	% Recovery
Sample -1	3.0	2.68 ± 0.01	3.12 ± 0.40	104.39
Sample -2	5.0	5.04 ± 0.01	5.20 ± 0.55	107.93
Sample -3	7.0	6.93 ± 0.01	7.21 ± 1.26	96.09

Conclusions

The nanofibers containing cellulose acetate as the supporting natural polymer and rhodamine hydrazone derivative **L1** as the coloring agent, was successfully fabricated by electrospinning and subsequently utilized for Cu^{2+} sensing in aqueous samples by naked-eye detection. The color of the membrane changed from pale-pink to intense pink color as a result of the formation of **CuL1** product. The effects of amount of **L1**, pH and response time were investigated. The nanofibrous sensor can detect Cu^{2+} in water samples displayed good sensitivity, selectivity and the detection limit for Cu^{2+} with **L1-CA** nanofibers was found to be 1.62 mg L^{-1}.

Acknowledgements

This work was financially supported by The Promotion of Science and Mathematics Talent Teacher (PSMT).

References

Ahuja, A., Dev, K., Tanwar, R. S., Selwal, K. K., & Tyagi, P. K. (2015). Copper mediated neurological disorder: Visions into amyotrophic lateral sclerosis, Alzheimer and Menkes disease. *Journal of Trace Elements in Medicine and Biology, 29*, 11-23.

Alia, R., Elshaarawy, R. F.M., & Saleh, S. M. (2017). Turn-on ratiometric fluorescence sensor film for ammonia based on salicylaldehyde-ionic liquid. *Journal of Environmental Chemical Engineering, 5,* 4813 - 4818.

Busaranon, K., Suntornsuk, W., & Suntornsuk, L. (2006). Comparison of UV spectrophotometric method and high performance liquid chromatography for the analysis of flunarizine and its application for the dissolution test. *Journal of Pharmaceutical and Biomedical Analysis, 41*, 158–164.

Chandran, R., Chevva, H., Zeng, Z., Liu, Y., Zhang, W., Wei, J., & LaJeunesse, D. (2018). Solid-state synthesis of silver nanowires using biopolymer thin films. *Materials Today Nano, 1*, 22-28.

Chen, B.-Y., Kuo, C.-C., Huang, Y.-S., Lu, S.-T., Liang, F.-C., & Jiang, D.-H. (2015). Novel Highly selective and reversible chemosensors based on dual-ratiometric fluorescent electrospun nanofibers with pH- and Fe3+-Modulated Multicolor Fluorescence Emission. *ACS Applied Materials & Interfaces, 7*, 2797-2808.

Chen, X., Pradhan, T., Wang, F., Kim, J. S., & Yoon, J. (2012). Fluorescent chemosensors based on spiroring-opening of xanthenes and related derivatives. *Chemical Reviews, 112*, 1910-1956.

Crichton, R. R., Dexter, D. T., & Ward, R. J. (2008). Metal based neurodegenerative diseases—From molecular mechanisms to therapeutic strategies. *Coordination Chemistry Reviews, 252*, 1189-1199.

Eftekhari, A. (2003). pH sensor based on deposited film of lead oxide on aluminum substrate electrode. *Sensors and Actuators B: Chemical, 88*, 234-238.

Eftekhari, E., Wang, W., Li, X., A, N., Wu, Z., Klein, R., Cole, I. S., & Li, Q. (2017). Picomolar reversible Hg(II) solid-state sensor based on carbon dots in double heterostructure colloidal photonic crystals. *Sensors and Actuators B: Chemical, 240*, 204-211.

Flores, E., Pizarro, J., Godoy, F., Segura, R., Gómez, A., Agurto, N., & Sepúlveda, P. (2017). An electrochemical sensor for the determination of Cu(II) using a modified electrode with ferrocenyl crown ether compound by square wave anodic stripping voltammetry. *Sensors and Actuators B: Chemical, 251*, 433-439.

Fu, X.-C., Wu, J., Xie, C.-G., Zhong, Y. & Liu, J. –H. (2013) Rhodamine-based fluorescent probe immobilized on mesoporous silica microspheres with perpendicularly aligned mesopore channels for selective detection of trace mercury(II) in water. *Anal. Methods*, *5*, 2615-2622.

Hu, L., Yan, X. W., Li, Q., Zhang, X. J., & Shan, D. (2017). Br-PADAP embedded in cellulose acetate electrospun nanofibers: Colorimetric sensor strips for visual uranyl recognition. *Journal of Hazardous Materials, 329*, 205-210.

Jensen, P. Y., Bonander, N., Møller, L. B., & Farver, O. (1999). Cooperative binding of copper(I) to the metal binding domains in Menkes disease protein. *Biochimica et Biophysica Acta, 1434*, 103-113.

Rull-Barrull, J., Grognec, M. H. E., & Felpin, F. –X. (2016) Chemically-modified cellulose paper as smart sensor device for colorimetric and optical detection of hydrogen sulfate in water. *Chemical Communications*, *52*, 2525-2528.

Kim, H. N., Lee, M. H., Kim, H. J., Kim, J. S., & Yoon, J. (2008). A new trend in rhodamine-based chemosensors: application of spirolactam ring-opening to sensing ions. *Chemical Society Reviews, 37*, 1465-1472.

Li, M., Li, X., Xiao, H.-N., & James, T. D. (2017). Fluorescence Sensing with Cellulose-Based Materials. *Chemistry Open, 6*, 685 – 696.

Liu, Y., Liang, P., & Guo, L. (2005). Nanometer titanium dioxide immobilized on silica gel as sorbent for preconcentration of metal ions prior to their determination by inductively coupled plasma atomic emission spectrometry. *Talanta, 68*, 25-30.

McDonagh, C., Burke, C. S., & MacCraith, B. D. (2008). Optical chemical sensors. *Chemical Reviews, 108*, 400-422.

Miotto, M. C., Rodriguez, E. E., Valiente-Gabioud, A. A., Torres-Monserrat, V., Binolfi, A., Quintanar, L., Zweckstetter, M., Griesinger, C., & Fernández, C. O. (2014). Site-Specific Copper-Catalyzed Oxidation of α-Synuclein: Tightening the Link between Metal Binding and Protein Oxidative Damage in Parkinson's Disease. *Inorganic Chemistry, 53*, 4350-4358.

Nunes, C. J., Borges, B. E., Nakao, L. S., Peyroux, E., Hardré, R., Faure, B., Réglier, M., Giorgi, M., Prieto, M. B., Oliveira, C. C., & Da Costa Ferreira, A. M. (2015). Reactivity of dinuclear copper(II) complexes towards melanoma cells: Correlation with its stability, tyrosinase mimicking and nuclease activity. *Journal of Inorganic Biochemistry, 149*, 49-58.

O'Halloran, T. V., & Culotta, V. C. (2000). Metallochaperones, an intracellular shuttle service for metal ions. *The Journal of Biological Chemistry, 275*, 25057-25060.

Ozay, H., & Ozay, Ozgur. (2013) Rhodamine based reusable and colorimetric naked-eye hydrogel sensors for Fe^{3+} ion. *Chem. Eng. J.*, *232*, 364-371.

Piriya V.S, A., Joseph, P., Daniel S.C.G, K., Lakshmanan, S., Kinoshita, T., & Muthusamy, S. (2017). Colorimetric sensors for rapid detection of various analytes. *Materials Science and Engineering: C, 78*, 1231-1245.

Pourreza, N., & Hoveizavi, R. (2005). Simultaneous preconcentration of Cu, Fe and Pb as methylthymol blue complexes on naphthalene adsorbent and flame atomic absorption determination. *Analytica Chimica Acta, 549*, 124-128.

Saithongdee, A., Praphairaksit, N., & Imyim, A. (2014). Electrospun curcumin-loaded zein membrane for iron(III) ions sensing. *Sensors and Actuators B: Chemical, 202*, 935-940.

Strausak, D., Mercer, J. F. B., Dieter, H. H., Stremmel, W., & Multhaup, G. (2001). Copper in disorders with neurological symptoms: Alzheimer's, Menkes, and Wilson diseases. *Brain Research Bulletin, 55*, 175-185.

Telianidis, J., Hung, Y. H., Materia, S., & La Fontaine, S. (2013). Role of the P-Type ATPases, ATP7A and ATP7B in brain copper homeostasis. *Frontiers in Aging Neuroscience, 5*, 1-17.

Terra, I. A. A., Mercante, L. A., Andre, R. S., & Correa, D. S. (2017). Fluorescent and colorimetric electrospun nanofibers for heavy-metal sensing. *Biosensors, 7*, 1-14.

Tokman, N. (2007). The use of slurry sampling for the determination of manganese and copper in various samples by electrothermal atomic absorption spectrometry. *Journal of Hazardous Materials, 143*, 87-94.

Wang, L., Ye, D., Li, W., Liu, Y., Li, L., Zhang, W., & Ni, L. (2017). Fluorescent and colorimetric detection of Fe(III) and Cu(II) by a difunctional rhodamine-based probe. *Spectrochimica Acta Part A: Molecular and Biomolecular Spectroscopy, 183*, 291–297.

Wang, W., Yang, Q., Sun, L., Wang, H., Zhang, C., Fei, X., Sun, M., & Li, Y. (2011). Preparation of fluorescent nanofibrous film as a sensing material and adsorbent for Cu^{2+} in aqueous solution via copolymerization and electrospinning. *Journal of Hazardous Materials, 194*, 185–192.

World Health Organization (2017). *Guidelines for drinking-water quality: fourth edition incorporating the first addendum*. Brazil

Wu, W.-C., & Lai, H.-J. (2016). Preparation of thermo-responsive electrospun nanofibers containing rhodamine-based fluorescent sensor for Cu^{2+} detection. *Journal of Polymer Research, 23*, 223-226.

Xiang, Y., Tong, A., Jin, P., & Ju, Y. (2006). New Fluorescent Rhodamine Hydrazone Chemosensor for Cu(II) with High Selectivity and Sensitivity. *Organic Letters, 8*, 2863-2866.

Zhang, X., Zhang, W., Li, C., & Li, Y. (2018) Facile self-assembly of pyromellitic acid modified graphene oxide sheets into rhodamine B for highly selective luminescent sensing of Fe^{3+}. *Journal of Alloys Compounds*, *749*, 503-510